ISIJ International, Vol. 48 (2008), No. 12, pp. 1704–1711

Modeling of Three-phase Flows and Behavior of Slag/Steel Interface in an Argon Gas Stirred Ladle

Baokuan LI,[1] Hongbin YIN,[2] Chenn Q. ZHOU[3] and Fumitaka TSUKIHASHI[4]

1) School of Materials and Metallurgy, Northeastern University, Shenyang, 110004, China.
2) Mittal Steel USA Research Center, East Chicago, IN 46312, USA. 3) Department of Mechanical Engineering, Purdue University Calumet, Hammond. IN 46321, USA. 4) Department of Advanced Materials, Graduate School of Frontier Science, The University of Tokyo, 5-1-5 Kashiwanoha, Kashiwa, Chiba 277-8561 Japan.

(*Received on April 17, 2008; accepted on September 9, 2008*)

A Mathematical model has been developed to analyze the transient three-dimensional and three-phase flow in an argon gas bottom stirring ladle with one and two off-centered porous plugs. Multiphase Volume of Fluid (VOF) method is used to simulate the behaviors of slag layer. Numerical simulation was conducted to clarify the transient phenomena of gas injection into the molten steel. When argon gas is injected into molten steel in a ladle, the gas rising passage is formed near the plug, and then bubbles are created in the molten steel. The rising gas bubbles impinge on the slag intermittently and break the slag layer to create the slag eye. Simultaneously, the wave at the slag–steel interface was formed and the wave frequency increases with the increase of argon gas flow rate for one off-centered plug case. The modeling simulations show that the diameter of slag eye changes from 0.43 to 0.81 m when the flow rate of argon gas varies from 100 to 300 NL/min for a 220 ton ladle. The relationship between non-dimensional areas of slag eye and the modified Froude number is in good agreement with the experimental data reported in literature. At the same total gas flow rate of 300 NL/min, the two-plugs generate two eyes with the diameters of around 0.6 m. Since the significant deformation of slag layer occurs during gas stirring operation, the thickness of slag becomes thin near the slag eye and thick near the ladle wall, respectively. The downward flow velocity of steel at the slag eye periphery may be affected significantly by flow rate of Ar gas. Therefore, when the downward flow velocity would be larger, the more emulsification of slag could be expected.

KEY WORDS: ladle metallurgy; slag layer behavior; three-phase flow; mathematical model.

1. Introduction

The ladle metallurgy furnace (LMF) is fully responsible for the process of homogenization of composition of alloy elements and temperature, deoxidation, desulphurization and removal of inclusion. Efficiency of desulphurization in LMF for the production of Advanced High Strength Steels depends essentially on the interaction between slag and steel created by argon stirring. The slag layer plays a crucial role in the refining of liquid steel in ladle metallurgy. To enhance the interaction between steel and slag and promote the desulfurization reaction, argon gas is often injected into molten steel through the top lance or bottom porous plug of ladle. In this process, gas bubbles formed in the molten steel move up to the slag–metal interface and finally reach the top layer of slag phase. The rising gas bubbles push the molten steel upward at local area, stir the slag/metal interface, and create the emulsification of slag into molten steel, which significantly increase the contact area between slag and steel and hence accelerate the desulfurization reaction. However, undesirable phenomena, such as entrainment of slag and pickup of oxygen and nitrogen may occur, which are detrimental to steel quality.

Hydrodynamics and the associated transport phenomena of three phase flows are of great practical significance for the production of clean steel. The physical phenomena involved during the crossing of bubbles through the interface are very complicated.[1] Beskow *et al.*[2] develop a sampler to observe the physical description of the slag–metal interface in industrial trial experiments. Lachmund *et al.*[3] proposed a semi-empiric model to calculate the slag emulsification parameters. Han *et al.*[4] investigated the effect of oil layer on the flow pattern and mixing time in a gas stirred liquid bath. Jonsson *et al.*[5] had developed a two-dimensional fluid flow model combined with the thermodynamics of reoxidation and desulphurization. Even though a number of theories[6,7] have been proposed and developed to understand the behavior of slag–steel interface, the effect of gas stirring and other operating parameters on the slag–steel reaction is not clarified yet. Yonezawa and Schwerdtfeger[8] dealt with the spouts eye developed at the free surface of molten metal stirred by argon in the ladle. The cold model experiment in mercury bath and an oil layer as slag and also the industrial experiment with a 350 ton steel ladle had been carried out. The time average of free surface areas has been determined with dimensionless correlation. Krishnapisharody and Irons[9] measured eye sizes by the model experiments including the fluids to simulate slag and metal at a room tem-

© 2008 ISIJ

perature with various conditions such as gas flow rates, and depths of both fluids. A simulation model expressing a dimensionless eye area in terms of a density ratio of the fluids and Froude number has been developed.

A profound understanding of the motion of slag layer is increasingly felt as an essential requirement for today's steel industry to produce advanced high strength steels which require very low sulfur levels. The effect of slag layer is simplified or neglected in the previous model.[4–6] As the first stage to solve the problem, Ridenour *et al.*[1] had conducted a simulation study on the slag eye diameter and slag motion.

The purpose of the present study is the development of a mathematical model of a transient three-dimensional and three-phase flow in an argon gas bottom stirring ladle with one and two off-centered porous plugs. A preliminary quantitative analysis of the slag eye size is the second objective of the present study. Deformation behavior of slag layer is discussed based on the understanding of the behavior of slag/steel interface.

2. Mathematical Model

2.1. Governing Eequations

In order to investigate the dynamic behavior of three phase flow, VOF function[10] is used to express the reaction at the interface between molten steel and slag phases. The following governing transport equations including VOF function and turbulence model equations need to be solved.

Equation of Continuity

$$\frac{\partial \rho}{\partial t} + \nabla \cdot (\rho \vec{V}) = 0 \quad \text{.....(1)}$$

A single momentum equation is solved throughout the domain, and the resulting velocity field is shared among the phases. The momentum equation expressed as Eq. (2) is dependent on the volume fractions of all phases through the properties ρ and μ.

$$\frac{\partial}{\partial t}(\rho \vec{v}) + \nabla \cdot (\rho \vec{v}\vec{v}) = -\nabla p + \nabla \cdot [\mu_e (\nabla \vec{v} + \nabla \vec{v}^{\mathrm{T}})] + \rho \vec{g} \quad \text{.....(2)}$$

One limitation of the shared-fields approximation is that in cases where large velocity differences exist between the phases, the accuracy of the velocities computed near the interface can be adversely affected.

The VOF formulation relies on the fact that two or more fluids or phases are not interpenetrating. For each additional phase, a new variable is introduced such as the volume fraction of the phase in the computational cell. In each control volume, the sum of volume fractions of all phases is unity. The fields for all variables and properties are shared by the phases and represent volume-averaged values, as long as the volume fraction of each of the phases is known at each location. Thus the variables and properties in any given cell are either purely representative of one of the phases, or representative of a mixture of the phases, depending upon volume fraction values.

$$\alpha_{\mathrm{gas}} + \alpha_{\mathrm{steel}} + \alpha_{\mathrm{slag}} = 1 \quad \text{.....(3)}$$

In other words, if the q th fluid's volume fraction in the cell is denoted as α_q, then the following three conditions are possible:

- $\alpha_q = 0$: the cell is empty (of the qth fluid).
- $\alpha_q = 1$: the cell is full (of the qth fluid).
- $0 < \alpha_q < 1$: the cell contains the interface between the qth fluid and one or more other fluids.

The volume-fraction-averaged density takes on the following form:

$$\rho = \alpha_{\mathrm{gas}}\rho_{\mathrm{gas}} + \alpha_{\mathrm{steel}}\rho_{\mathrm{steel}} + \alpha_{\mathrm{slag}}\rho_{\mathrm{slag}} \quad \text{.....(4)}$$

The volume-fraction-averaged viscosity is computed in this manner.

$$\mu = \alpha_{\mathrm{gas}}\mu_{\mathrm{gas}} + \alpha_{\mathrm{steel}}\mu_{\mathrm{steel}} + \alpha_{\mathrm{slag}}\mu_{\mathrm{slag}} \quad \text{.....(5)}$$

The VOF function α_q satisfies Eq. (6).

$$\frac{\partial \alpha_q}{\partial t} + (\vec{v} \cdot \nabla)\alpha_q = 0 \quad \text{.....(6)}$$

The standard k–ε model is used to calculated effective viscosity with including the effect of buoyancy:

$$\frac{\partial}{\partial t}(\rho k) + \frac{\partial}{\partial x_i}(\rho k u_i) = \frac{\partial}{\partial x_j}\left[\left(\mu + \frac{\mu_t}{\sigma_k}\right)\frac{\partial k}{\partial x_j}\right] + G_k + G_b - \rho\varepsilon \quad \text{....(7)}$$

and

$$\frac{\partial}{\partial t}(\rho \varepsilon) + \frac{\partial}{\partial x_i}(\rho \varepsilon u_i) = \frac{\partial}{\partial x_j}\left[\left(\mu + \frac{\mu_t}{\sigma_\varepsilon}\right)\frac{\partial \varepsilon}{\partial x_j}\right] + C_{1\varepsilon}\frac{\varepsilon}{k}(G_k + C_{3\varepsilon}G_b) - C_{2\varepsilon}\rho\frac{\varepsilon^2}{k} \quad \text{.....(8)}$$

In these equations, G_k represents the generation of turbulence kinetic energy due to the mean velocity gradients and this term may be defined as Eq. (9).

$$G_K = -\rho\overline{u_i' u_j'}\frac{\partial u_j}{\partial x_i} \quad \text{.....(9)}$$

The term G_b is the generation of turbulence kinetic energy due to buoyancy and calculated by Eq. (10).

$$G_b = -g_i\frac{\mu_t}{\rho \mathrm{Pr}_t}\frac{\partial \rho}{\partial x_i} \quad \text{.....(10)}$$

The turbulent or eddy viscosity, μ_t, is computed by combining k and ε according to Eq. (11).

$$\mu_t = \rho C_\mu \frac{k^2}{\varepsilon} \quad \text{.....(11)}$$

where C_μ is a constant, and $C_{1\varepsilon}=1.44$, $C_{2\varepsilon}=1.92$, $C_\mu=0.09$, $\sigma_k=1.0$, $\sigma_\varepsilon=1.3$, $C_{3\varepsilon}=1.0$.

2.2. Geometrical and Operational Conditions

The ladle studied in this work is a 220 ton ladle of No. 2

© 2008 ISIJ

Table 1. Geometrical, physical properties and operating parameters.

Parameters	value
Diameter of ladle in slag layer, m	3.32
Height of ladle, m	3.86
Depth of molten steel, m	3.26
Thickness of slag layer, m	0.05 to 0.15
Diameter of plugs, m	0.15
Eccentricity of plugs, m	0.5
Flow rate of argon gas, *Nl*/min	100 to 300
Density of molten steel, kg/m^3	7020
Viscosity of molten steel, m^2/s	0.006
Density of slag, kg/m^3	3500
Viscosity of slag, m^2/s	0.03
Density of argon gas, kg/m^3	0.568
Viscosity of argon gas, m^2/s	8.535×10^{-5}

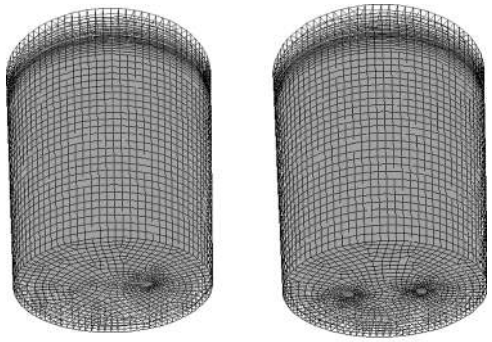

Fig. 1. Geometries and meshes of ladles with one and two bottom plugs.

Steel Works, Arcelor Mittal USA Indiana Harbor Works, where most of the advanced high strength steels are produced. Input conditions such as geometrical, thermo-physical properties and operating parameters are shown in **Table 1**. **Figure 1** displays the actual ladle geometries with one and two off-centered plugs.

2.3. Initial and Boundary Conditions

Initially, the steel bath starts at rest with no argon blowing through the porous plug. The slag layer rests on top of the steel bath. Since the heat transfer is not in the scope of this simulation research, temperature stratification in steel bath is neglected. It was assumed that the walls in the ladle are smooth and non-slip, which assumption makes easy for meshing. The inlet velocity of argon gas is calculated by the flow rates of argon gas by Eq. (12).

$$V_{in} = \frac{Q_L}{A} = \left(\frac{p_S T_L}{p_L T_S}\right)\frac{Q_S}{A} \quad \text{.....(12)}$$

where, subscript L means ladle operating condition, and S is standard condition. T_S=298 K, T_L=1 873 K, p_S=1 atm, and $p_L=p_S+\rho gH$. A is plug area, and Q_S is argon gas flow rate at standard condition as shown in Table 1. The boundary values for k and ε at ladle porous plugs are calculated with Eq. (13).

$$k_{in} = 0.04V_{in}^2, \quad \varepsilon_{in} = 2k^{3/2}/D_{plug} \quad \text{.....(13)}$$

The hydraulic diameter is same as the plug diameter. The free surface of the slag/argon gas interface is frictionless. An allowance is made for the escape of gas bubbles at the interface.

2.4. Numerical Method

The solutions of the governing equations with boundary conditions and source terms are obtained using the commercial fluid dynamics package Fluent. The calculation domain is divided by the 46 848 nodes for one plug and 59 040 nodes for two plugs. The calculations are conducted in the unsteady solution mode using the SIMPLE algorithm to solve the three phase flow problem. A criterion for convergence in all cases simulated in the present study is established when the sum of all residuals for the dependent variables is less than 10^{-4}. A typical calculation for the simulation for 90 s with the conditions of starting zero velocity field and time step of 0.01 s required 100 h computational time by using P4 CPU 3.6 GHz and 2.00 GB of RAM.

3. Results and Discussion

Generally, one off-center plug is used to inject the argon gas into the steel bath. The variables for three-phase flow simulation include the phase distribution, velocity field and turbulent kinetic energy *etc.* The conditions for base case are flow rate of argon gas injection of 200 NL/min, and one off-center plug and slag thickness of 100 mm.

3.1. Phase Interface Configuration

Distributions of three phases such as argon gas, steel and slag are displayed in **Figs. 2** to **4**. Argon gas plume is formed above the plug at bottom of ladle. When the gas is injected into the ladle, the dynamic pressure of gas is more than the pressure head due to the depth of liquid. Therefore, there is a blow-through distance, which is a gas jet that initially enters the liquid and is called "gas jet core". Although the diameter of each pore in porous plug is small, large quantity of pores are used in the immediate vicinity. Since the effect of the porous plug on the gas blow-through is equivalent to the nozzle, the jet core is formed adjacent to the plug, and bubbles are created in the molten steel as shown in Fig. 2. As the argon gas bubbles impinge the slag intermittently, the wave at interface of slag–steel is formed. As the result of upwelling flow in the gas plume, the configuration of molten steel surface at interface between slag and steel is displayed in Fig. 3, where the spout peak of upwelling flow can be clearly observed. Figure 4 exhibits the deformation of slag layer on main section at 41 s. The thickness of slag becomes thin near the slag eye and thick near the ladle wall. As the flows are unsteady, these configurations of phase interface are transient phenomena.

The calculated flow field at main section for all zones including gas, steel and slag phases is shown in **Fig. 5**. The flow pattern under the slag is accordance with the previous

© 2008 ISIJ

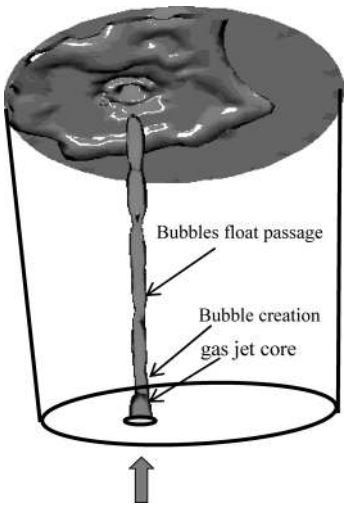

Fig. 2. Interface configuration of argon gas and molten steel.

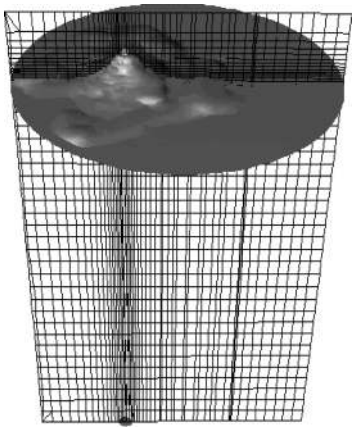

Fig. 3. Interface configuration between molten steel and slag.

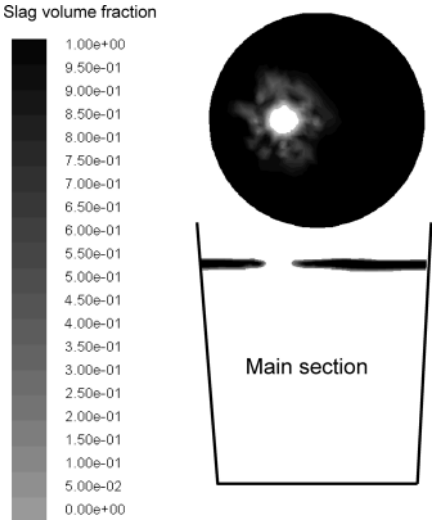

Fig. 4. Slag layer distribution at main section of a ladle.

results.[11–13] Nevertheless, flow pattern near the slag layer is very complex, and some vortices appear as shown in **Fig. 6**. Variation of flow patterns are caused by the difference of physical properties between slag and steel.

3.2. Slag Layer Behavior

Since the efficiency of desulphurization in LMF process

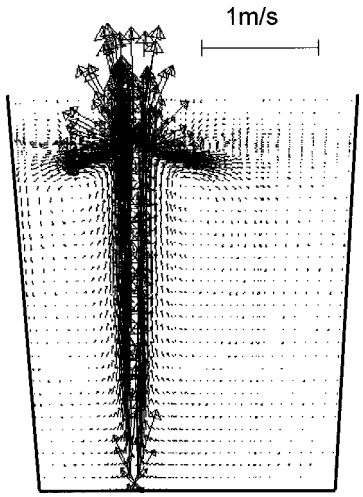

Fig. 5. Velocity distribution at main section of the bottom gas stirring ladle at 41 sections.

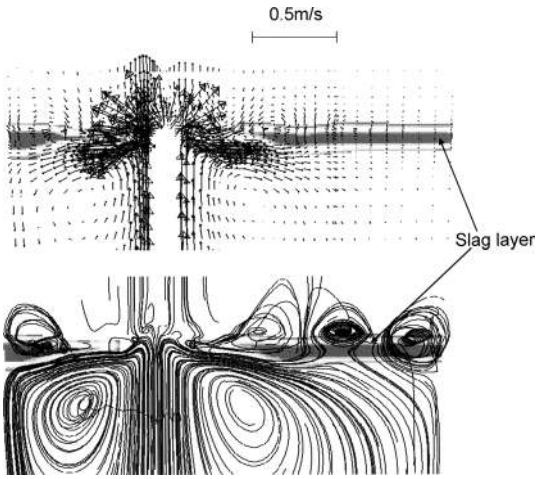

Fig. 6. Velocity distribution near slag/steel interface.

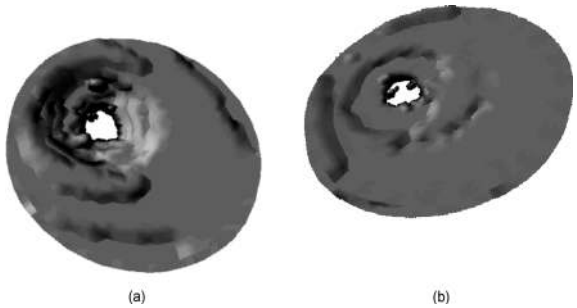

Fig. 7. Interface configuration of slag layer at 41 s, (a) interface of slag/steel, and (b) surface of slag layer.

depends significantly on the interaction behavior between slag and steel created by argon stirring, it is important to make clear the interaction behavior. **Figure 7** displays the surface profile of the slag layer at (a) the interface between slag and steel and (b) top surface. Rugged surface is produced due to the collision of rising bubbles that enlarges the interface area.

More significant aspect of the increase of slag/steel interface is the emulsification of slag into liquid steel caused by the strong shear force from fast steel flow around the slag eye. Although currently it is not possible to quantify the slag emulsification process through the CFD modeling,

© 2008 ISIJ

three characteristics of the slag/steel interface can be used as indicators of the magnitude of the emulsification. They are (1) the liquid steel velocity at the periphery of the eye, (2) the length of the slag eye periphery, *i.e.* the size of the eye and (3) the interface wave frequency.

Larger interface velocity can promote more emulsification and formation of more slag/steel contact area for fast reaction. The interface velocity is given in **Figs. 8**(a) and 8(b), where are viewed at the same direction as Fig. 7. The interface velocity at the boundary of the slag eye in Fig. 8(a) is heading downwards at very high magnitude. Because the viscosity of slag and interface tension between slag and molten steel are large, it needs a large momentum for steel to overcome the slag tension and viscous force in slag eye. This strong flow which velocity directions are downward in slantways may drag the slag into the steel to generate enormous emulsification. The time averaged velocity rates at eight points uniformly around slag eye periphery at 41 s are shown in **Fig. 9**. The effect of argon gas flow rates on velocity at interface between slag and steel is significant. The downward steel flow velocity is about 3 times higher for Ar flow rate of 300 NL/min than for 100 NL/min.

A bigger size of slag eye will give a longer eye periphery and hence more slag volume to get involved in the emulsification process. To obtain the length of the slag eye periphery, an estimation of the peak of Ar/steel spout is necessary. From the viewpoint of chemical reaction rate, the spout peak height is also an important index of reaction in ladle metallurgy process. The effect of injection flow rate of argon gas on the spout peak height is shown in **Fig. 10**. Generally, the height of spout peak based on datum line at slag–steel interface should be more than the slag thickness to create enough slag eye size. **Figure 11** shows the effect of argon gas flow rate on the diameter of slag eye. At

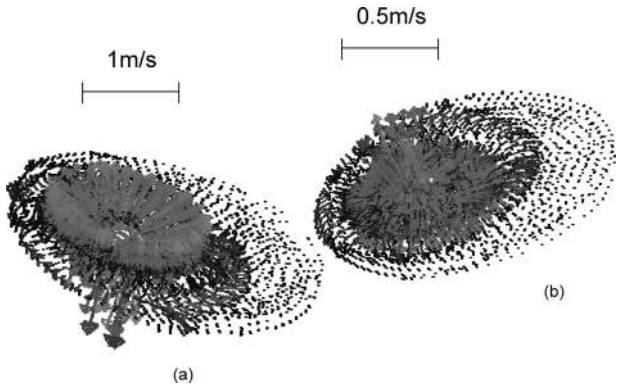

Fig. 8. Interface velocities of slag layer at 41 s, (a) interface of slag/steel and (b) interface of slag/argon gas.

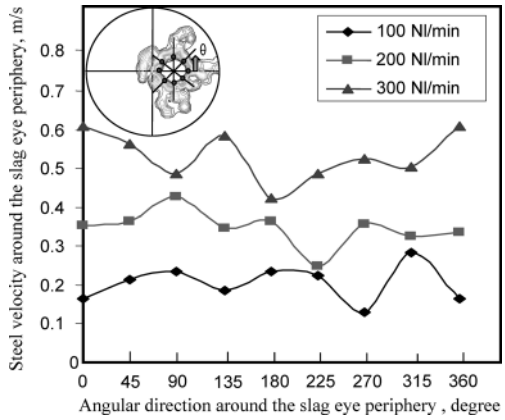

Fig. 9. Effect of argon gas flow rate on steel velocity around the slag eye periphery.

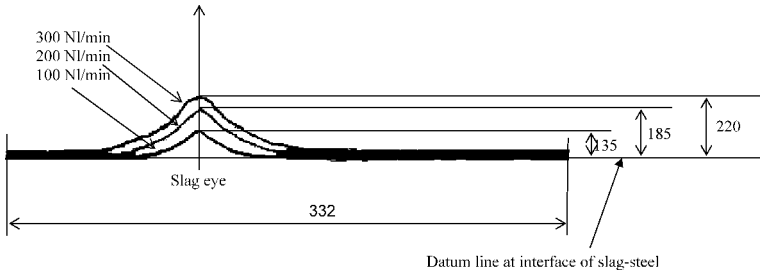

Fig. 10. Effect of argon gas flow rate on the spout height in the slag/steel interface.

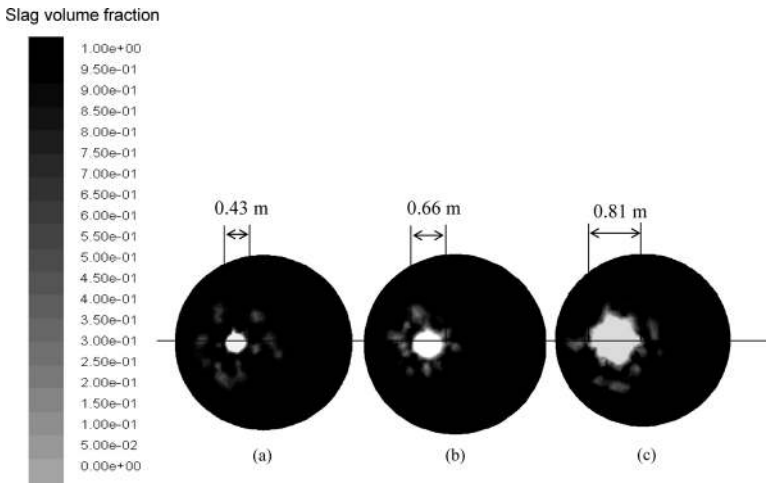

Fig. 11. Variation of slag eye area with the argon gas flow rate (a) 100 NL/min, (b) 200 NL/min, and 300 NL/min.

© 2008 ISIJ

100 mm slag thickness, Ar flow rate of 200 NL/min can generate a slag eye in diameter of about 660 mm which gives a 2.1 m long slag periphery for slag emulsification, the eye diameter is only 430 mm and the slag periphery is about 1.35 m when Ar flow rate is set at 100 NL/min.

Yonezawa and Schwerdtfeger,[9] and Krishnapisharody and Irons,[8] have measured the eye size in room-temperature model and actual steel ladle operations. These various data can be expressed by plotting the modified Froude number (Fr_D) defined by $(\rho/\Delta\rho)(u^2/gh)$ against the nondimensional area (A_e/H^2) as shown in **Fig. 12**. Results of the present work are also shown in this Fig. 12. It indicates that the slag eye areas obtained by the present model may be somewhat less than actual ones.

The wave formation at slag/steel interface is another important factor for slag emulsification. It is known that the wave frequency becomes larger, the slag at the eye periphery is easier to break up into smaller pieces and be dragged deeper into steel stream. The variation of wave frequency with the flow rate of argon gas is shown in **Fig. 13**. The frequency increases with the increase of argon gas flow rate, since higher flow rate produces a mass of gas bubbles in molten steel.

From this simulation, it can be clarified that the Ar flow rate should have a significant effect on slag emulsification through the contributions of higher slag eye periphery velocity, longer periphery length and higher the slag/steel interface wave frequency. In other words, higher efficiency of the desulfurization can be achieved at higher Ar flow rate. Future work will focus on quantification of the slag emulsification process and correlate these three factors to apply for the commercial desulfurization operations.

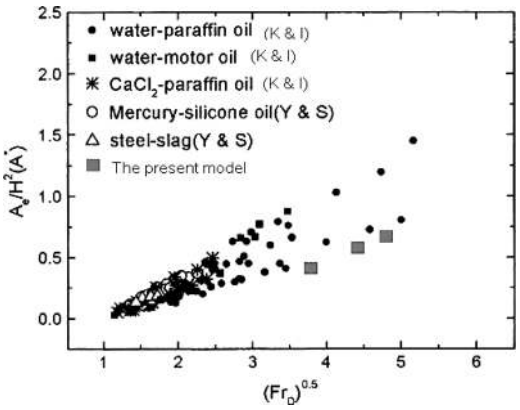

Fig. 12. Nondimensional eye area vs modified Froude number (K&I: Krishnapisharody and Irons[9]; Y&S: Yonezawa and Schwerdtfeger[8]).

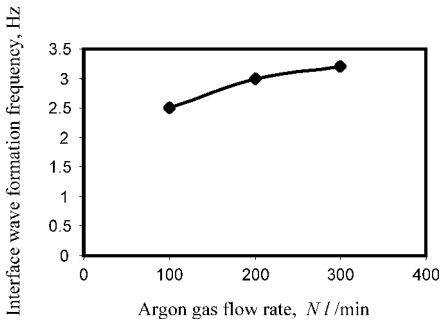

Fig. 13. Effect of argon gas flow rate on the interface wave frequency of slag/steel, one plug placed off-centrally.

3.3. Effect of Nozzle Number

When two plugs are used at the symmetrical location of one off-centered plug, the argon gas flow rate is equally divided into two parts. Argon gas volume of fraction is shown in **Fig. 14**. The time that the gas bubbles reach to the slag layer in the case of two plugs type is longer than that in the case with one plug type, because there is an approximately symmetrical flow pattern around centerline under the slag layer as shown in **Fig. 15**. The rising of gas bubbles is restricted by downward flow of another gas plume.

Figure 16 shows the more complicated vortices system in the region of slag layer, which is produced by the differ-

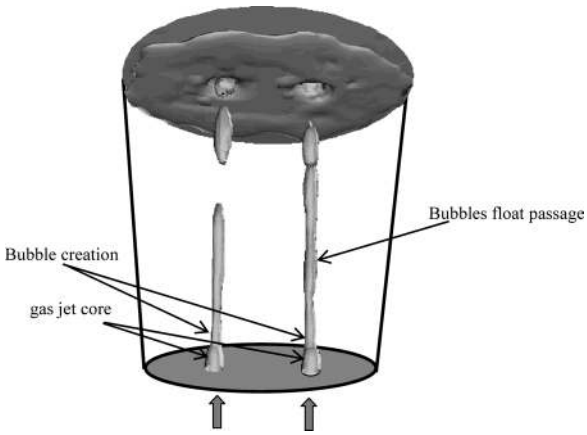

Fig. 14. Interface configuration of argon gas and molten steel in a ladle with two plugs.

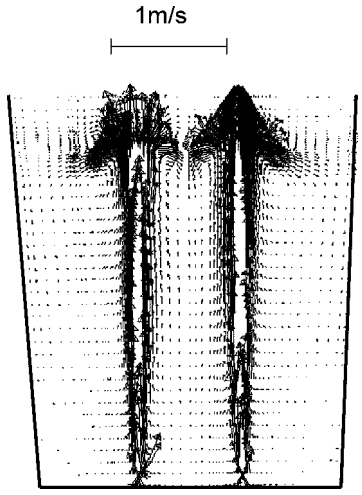

Fig. 15. Flow field at main section of a gas stirring ladle with two bottom plugs.

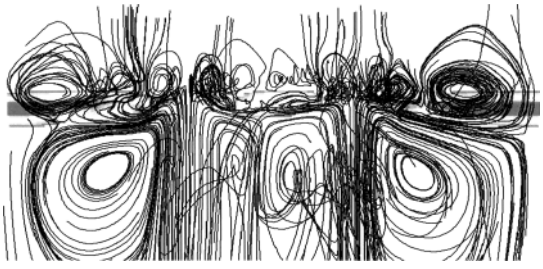

Fig. 16. Path lines in flow field near the zone of slag layer.

© 2008 ISIJ

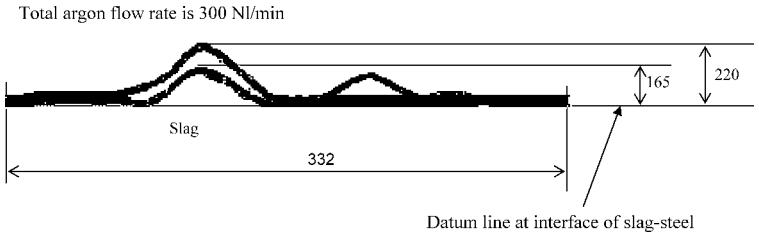

Fig. 17. Comparison of molten steel spout height between one and two plugs, unit=mm.

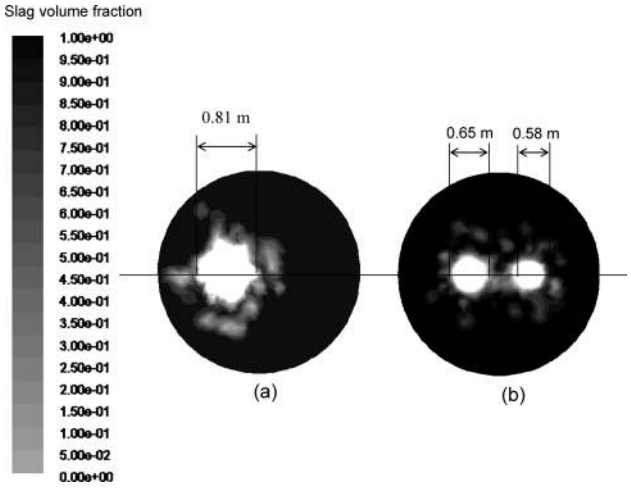

Fig. 18. Comparison of slag eye areas between (a) one plug and (b) two plugs in case that argon gas flow rate is 300 NL/min.

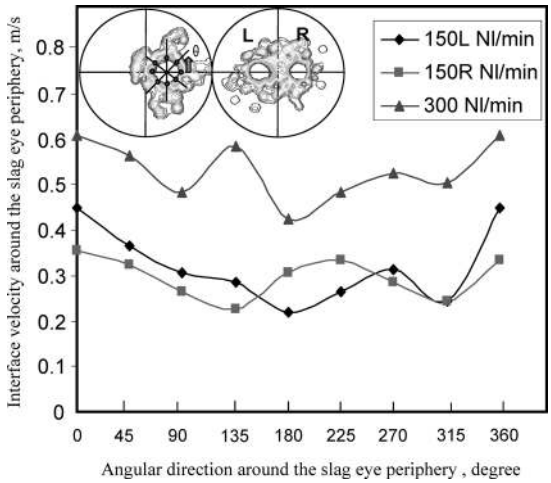

Fig. 19. Comparison of interface velocity around the slag eye periphery between one and two plugs.

ent physical properties of three phase and non-uniform external effects. Comparison of spout peak height of molten steel between one and two plugs operations is shown in **Fig. 17**, and sum of two slag eye areas is larger than that of one plug as shown in **Fig. 18**. The slag eye periphery length for one plug is 2.5 m compared with 3.9 m for 2 porous plugs. On the other hand, the downward flow velocity of steel at the slag eye periphery for two plugs is smaller than that for the one plug case as illustrated in **Fig. 19**. Therefore, these two effects on slag emulsification may be cancelled. In addition, the wave formation is much more complicated for the two plugs case than the one plug case due to interaction between the two raising plumes on the surface. More work is necessary to evaluate the interface wave formation on slag emulsification. Currently, it is not yet possible to clarify if two-plug system is better than one-plug system in terms of slag emulsification.

4. Conclusions

(1) Numerical simulation was conducted for the transient phenomena of gas injection into the ladle. When argon gas is injected into molten steel in a ladle, gas plume is formed above the plug, and then bubbles are moved into the molten steel. The rising gas bubbles impinge the slag intermittently and breakthrough the slag layer to create the slag eye. Simultaneously, the wave was formed at slag–steel interface.

(2) The injection flow rate of Argon gas has an effect on the spout peak height and the area of slag eye. The diameter of slag eye changes from 0.43 m to 0.81 m for 220 ton ladle while the flow rate of argon gas varies from 100 to 300 NL/min. The obtained relationship between non-dimensional areas of slag eye and the modified Froude number is in good agreement with the reported data. At the same total gas flow rate of 300 NL/min, the two-plugs generate two eyes with the diameters at about 0.6 m.

(3) Significant deformation of slag layer occurs during gas stirring operation, and the thickness of slag becomes thin near the slag eye and thick near the ladle wall, respectively. The more complicated vortices in the slag layer were observed by simulation, which is produced by the different physical properties of three phase and non- uniform external effects.

(4) The downward flow velocity of steel at the slag eye periphery was significantly affected on the Ar gas flow rate. When the velocity of steel becomes larger, the more slag emulsification can be expected.

Acknowledgements

One of the authors, Baokuan Li, is grateful to the National Natural Science Foundation of China and Baosteel Co., Ltd. for support of this research, Grant No. 50774111.

REFERENCES

1) P. Ridenour, H. Yin, S. R. Balajee, P. Chaubal and C. Q. Zhou: AIST Iron & Steel Technology Conf. Proc., ed. by R. E. Ashburn, AIST, Warrendale, PA, (2006), 721.
2) K. Beskow, P. Dayal, J. Bjorkvall, M. Nzotta and D. Sichen: *Ironmaking Steelmaking*, **33** (2006), 74.
3) H. Lachmund, Y. K. Xie, T. Buhles and W. Pluschkell: *Steel Res. Int.*, **74** (2003), 77.
4) J. W. Han, S. H. Heo, D. H. Kam, B. D. You, J. J. Park and H. S. Song: *ISIJ Int.*, **41** (2001), 1165.
5) L. Jonsson, C. E. Grip, A. Johansson and P. Jonsson: Steelmaking

© 2008 ISIJ

Conf. Proc., ed. by R. E. Ashburn, ISS, Warrendale, PA, (1997), 69.
6) L. Jonsson and P. Jonsson: *ISIJ Int.*, **36** (1996), 1127.
7) A. Margareta, T Andersson, L. Jonsson and P. Jonsson: *ISIJ Int.*, **40** (2000), 1080.
8) K. Yonezawa and K. Schwerdtfeger: *Metall. Mater. Trans. B*, **30B** (1999), 411.
9) K. Krishnapisharody and G. A. Irons: *Metall. Mater. Trans. B*, **37B** (2006), 763.
10) C. W. Hirt and B. D. Nichols: *J. Comput. Phys.*, **39** (1981), 201.
11) B. Li, J. He and Z. Lu: *Acta Metall. Sin.*, **6B** (1993), 173.
12) D. Mazumdar and R. I. L. Guthrie: *ISIJ Int.*, **35** (1995), 1.
13) D. Mazumdar and R. I. L. Guthrie: *Metall. Mater. Trans. B*, **25B** (1995), 308.

© 2008 ISIJ